Journal of Scientific & Industrial Research
Vol. 84, September 2025, pp. 957-970
DOI: 10.56042/jsir.v84i9.5873

Intelligent Approach for Analysing and Forecasting Land Changes using Multispectral Images

Eliza Femi Sherley S[1], Shiloah Elizabeth Darmanayagam[1]* & Sunil Retmin Raj Cyril Raj[2]

[1]Department of Computer Science and Engineering, College of Engineering Guindy Campus, Anna University, Chennai 600 025, Tamil Nadu, India

[2]Department of Information Technology, Madras Institute of Technology Campus, Anna University, Chennai 600 044, India

Received 27 September 2023; revised 20 September 2024; accepted 02 September 2025

Monitoring the changes in land over time is useful to understand the impacts of human activities in the environment. Urban change detection using satellite images plays a major role in research on global environmental change identification and management of natural resources. With availability of multi-temporal satellite data, the proposed work aims to analyse the change on land in Indian regions. This work groups the regions of land with a Firefly Algorithm based clustering approach, which optimizes the cluster center identification process when compared to a conventional clustering approach, as a process of analysing changes with available multi-temporal data. Based on the vegetation, water, and built-up index values, clusters are labelled into appropriate land regions. The extent of change is then assessed using spatio-temporal information available and this helps to identify the pattern of change. Moreover, a deep learning technique, namely Regression-Long Short Term Memory (LSTM) network, is used to forecast future changes, which may be useful in managing urban resources. Understanding how the land has changed in the past, present, and predicted changes in the future may help in making right decisions. Experiments are carried out on Landsat 8 data from the Indian region to identify changes in land using unsupervised learning techniques. A Silhouette index of 0.88 was obtained on average by K-means clustering with three clusters, while 0.93 was obtained using Firefly integrated K-means clustering. Future land image forecasts generated by LSTM are compared to the actual image using the Structural Similarity Index (SSIM) and Root Mean Square Error (RMSE), resulting in SSIM of 0.85 and RMSE of 0.41 when the forecasted spectral band images are stacked into a multispectral image, indicating the effectiveness of the forecasting approach.

Keywords: Change detection, Clustering, Land cover, Land use, Regression

Introduction

Human beings, since the most basic stage of settlement, are reliant on land for their activities like agriculture (food activities), urbanisation and other sorts of commercial expansion which have been constantly transforming the universal landscape. The constant need to meet the requirements of the rapidly expanding population, as well as demand-driven progress activities, has put more stress on the earth's land. Use of land resources by the society gives rise to "land use" which varies with the purpose it serves for human needs and environmental features[1], the physical condition of the ground surface, including its quantity and composition (such as water, plants, and other earth components), is referred to as land cover.

By various studies, it is noted that considerable amount of land used for agriculture, land cover with water resources, forest areas are getting vanished due to rapid changes happening globally. Multi-temporal images are analysed to identify the changes in land by means of remote sensing or Geographic Information System (GIS) approaches. Statistics based on spatiotemporal dynamics of land use and land cover have been an effective measure to maintain the integrity of environmental components which helps in urban planning and management tasks.

Satellite images integrated with GIS data have been broadly used and recognized as a powerful mechanism to analyse the changes of land because of biological/human activities. Analysing the information of satellite data over period of time will provide details about what and where changes happened in land. Land details can be analysed using pixel based / object based information to estimate the rate of change that occurred over period of time.

To improve the development of natural resources, the pattern of land change should be recognized and thoroughly examined. With the Land use and Land Cover (LULC) change information that is detected,

*Author for Correspondence
E-mail: shiloah@annauniv.edu

the changes yet to happen in near future and what impact it would make with environmental and climate change in earth can be predicted.[2–4] Multiple sources of information such as temporal, spatial and non-spatial data are considered to be more important to analyse the land attributes and detect the changes.

To evaluate the land attributes, land cover and land use information is mapped in each temporal satellite image. The acquired multispectral and temporal satellite images are processed to get the reliable data for analysing land use and land cover information. Pixel based information are extracted to categorize the land where the enhanced clustering approach has been applied to overcome local convergence problem. Then these separated regions are categorized into water area, land and vegetation, etc.[5–7] In order to control land cover change and urban planning, the areas of multi-temporal images are analysed to ascertain the rate of change.

The proposed work focuses in analysing the changes in land from multispectral images collected over a specific period of time, and predict the changes in the near future in a particular geographic location. To identify the land changes over a time period land regions are first grouped using an enhanced clustering technique named Firefly integrated K-means clustering algorithm and then they are categorized according to the land information. Examining the changes that have occurred in a particular geographical location provides a clear view to identify and manage the land resources to take effective measures to protect the environment. The proposed work identifies the changes over land and also forecast the changes which might happen in near future using Regression-Long Short Term Memory (LSTM) technique which remains helpful for many socio-environmental applications. This work is generally focused on grouping the land by enhancing the clustering approaches which yields significant improvement in results while detecting and predicting changes in land. This work contributes for the research on land use and land cover monitoring by understanding the impacts of urbanization and natural resource management. By integrating geo-spatial data and machine learning approaches, this work focuses on detecting long-term changes in urban areas over a period of time and forecasting the land patterns in near future which are essential for sustainable land management. The proposed work with the predictive modelling, yields to offer practical solutions for environment-centric industries. Insights from this study can aid the industries and urban planners to identify the shifts in vegetation, water and land resources which assists them to anticipate the changes which might happen in near future. Consequently, by analysing the findings of this work, which mainly focus on Indian regions can guide the industries in making strategic decisions, to mitigate environmental risk and improve the planning of future developments in urban areas.

The succeeding sections of the manuscript are structured as follows. A comprehensive analysis of the related work is followed by the discussion of study area considered for this research and the system architecture of the proposed approach. Furthermore, the proposed methodology is described comprehensively. It further includes information about the configuration in which these experiments were carried out, as well as information about the bands processed in the dataset for land change analysis and a comparison with other existing methodologies. Eventually, the last Section concludes the LULC change analysis and forecasting and its future work.

Related Work

Analysis and identification of changes in land over time, both past and future, has long been a topic of debate in remote sensing. To summarise the research in this field, this section discusses supervised learning, unsupervised learning approaches to processing land regions, and optimization techniques used to improve the results of these approaches. Because satellite image data is large and identifying from-to changes is highly dependent on ground truth information such as a change map with detailed labels of changes, because the computational complexity of this process remains high, unsupervised approaches to land classification are preferred. The following is an overview of work in land change analysis and forecasting:

Islam *et al.*,[1] have proposed a method to assess land use changes by processing multispectral data using tools like ArcGIS v10.1 and ERDAS Imagine v14. Due to unavailability of quality imageries and existence of cloud cover in the input data, land use classification didn't turn out to be much efficient one. Clark[2] have presented a technique to classify and map the land cover classes in hyperspectral and multispectral imagery using Random Forest classifier and multiple end member mixture analysis classifier. Classification accuracy turns out to be better only for nine out of twelve land cover classes. Sundara *et al*.[3]

have proposed a method to predict land use and l and cover changes with Landsat 4-5(MSS-TM), Lands at7(ETM+SLC) and Landsat 8(OLI-TIRS) images using ERDAS imagine and Land Change Modeller of IDRISI Selva Software. The overall results obtained from this software were not efficient. Duong *et al.*[8] have proposed an automated classification approach which frame rules to classify land cover information. Each land cover class is assigned with a code along with the threshold values for Total Reflected Radiance Index (TRRI) and band ratio. Due to the seasonal change in data this approach faces difficulty and results with less accurate classification information. Shang *et al.*[9], discussed about how environmental variables are related to land cover (grass, forest, shrub, and barren) analysis, but uncertainties in the input datasets make this process to be challenging.

Li *et al.* [6] have proposed an approach which explores the information extraction methods which identify the feature patterns among remote sensing data in past decade. Over a period of time information is extracted through unsupervised, supervised learning techniques and un-mixing method. Uehara *et al.*[10] presented an automatic object detection approach for multispectral satellite data in which spatial and spectral features are extracted by multi-channel higher order local autocorrelation method. The authors used hierarchal Principal component analysis to eliminate the redundant which in turn improves the performance of object detection. Paul *et al.*[11] have introduced an approach to classify crop types from Surface reflectance of Landsat 8 data using normalized difference indices. Different feature selection and extraction approaches used for multispectral data are reviewed and evaluated for this study. Marnur *et al.*[12], discussed about unsupervised and supervised learning techniques to process satellite images and classify land cover information. Neogoe *et al.*[13], studied how the clustering algorithms are used to categorize remote sensing data. Taufik *et al.*[14], have presented a technique to classify the land using fuzzy rules. Standard Normalized Difference Water Index (NDWI), Normalized Difference Built-up Index (NDBI), and Normalized Difference Vegetation Index (NDVI) values are processed by adaptive neuro-fuzzy inference system which frame fuzzy rules to classify the land cover.

Senthilnath *et al.*[15] in their work have proposed an approach for solving problems in crop type classification from multispectral images using clustering approach which is integrated Bat Algorithm (BA). Optimal cluster centers were computed and validated on sample datasets from UCI repository. When compared to other metaheuristic techniques such as Genetic Algorithm (GA) and Particle Swarm Optimization (PSO), the BA is also more computationally efficient and can converge to solutions faster. Goel *et al.*[16] used multispectral images of the Saharanpur region outsourced from Defence Terrain & Research Lab (DTRL) of DRDO, India. They performed classification of the land regions as barren land, water and sparse vegetation by integrating cuckoo search and artificial bee colony algorithms. Joshil *et al.*[17] made a review on bio-inspired algorithm usage with classification techniques to increase the effectiveness and performance of classification with different bands of spectral data. Entire study is done with data of Alwar region, Rajasthan which is sourced from DTRL, a DRDO lab. According to experimental data, this review demonstrates that using a bio-inspired algorithm can improve classification accuracy and lower computational and time complexity. Nayak *et al.*[18] have proposed an improvisation for firefly algorithm by optimizing the weights set for the flashing behaviour of the fireflies using Pi Sigma Neural Network (PSNN). Improvised firefly algorithm is used to carry out classification task with Pima dataset, Balance dataset, and Heart dataset which is further validated using statistical tests like analysis of variance, Friedman, Dunnett and post hoc test, results of these indicate that this gives better solution. Goel *et al.*[19] presented a framework to extract efficient, focused and refined land cover features. Multispectral data of Alwar Area in Rajasthan, DTRL, DRDO is processed using Hybrid Ant Colony Optimization2 ACO2/PSO techniques which improvises the classifier for land cover feature extraction. Sharma *et al.*[5] has presented a study on optimization techniques like firefly algorithm and Particle swarm optimization for image classification with Radarsat-1 and Radarsat-2 data. Using meta-heuristic algorithms, feature optimization process is carried out to make classification results accurate and efficient one. For simulating the results in this study terrain features are considered as an input dataset, where kappa coefficient value is used to evaluate this method which gets higher value when compared with other conventional algorithms.

The input dataset obtained for processing land information contains a significant amount of uncertainty, according to a review of existing methods. Due to seasonal variations over time, certain

approaches encountered classification errors when labelling land. Unsupervised learning also had some issues with local convergence in fixing the cluster head, which had an impact on the effectiveness of clustering algorithms used to group the land. Due to the computational difficulty and lack of real-time open source data for examining change detection based on scene information, unsupervised learning-based change detection is preferred. This study proposes an enhanced clustering strategy that addresses the issue of local convergence and produces positive efficacy when grouping land areas.

Methodology

Study Area

The proposed work uses Landsat 8 data which is openly available in earth explorer provided by U.S. Geological Survey (USGS).[20] Datasets are downloaded by mentioning an appropriate geographical boundary for the study along with some other additional criterion to be mentioned such as zero percentage land cloud cover. Dataset can be exported along with all the metadata information such as product identifier, scene identifier details, ground control points and many other supportive information to process the satellite data. For this study, temporal image data from 2016 to 2019 were collected from urban regions specifically Chennai, India. The Study area map created using QGIS, visualizes the study area through a map of India, highlighting Tamilnadu. And also, the georeferenced Chennai district is presented in Fig. 1 to offer a clear understanding of study area. Dataset obtained from USGS lacks a ground truth mask for detecting temporal data changes. Manual labelling based on visual inspection of images leads to discrepancies when analysing land changes. As a result, with unlabelled

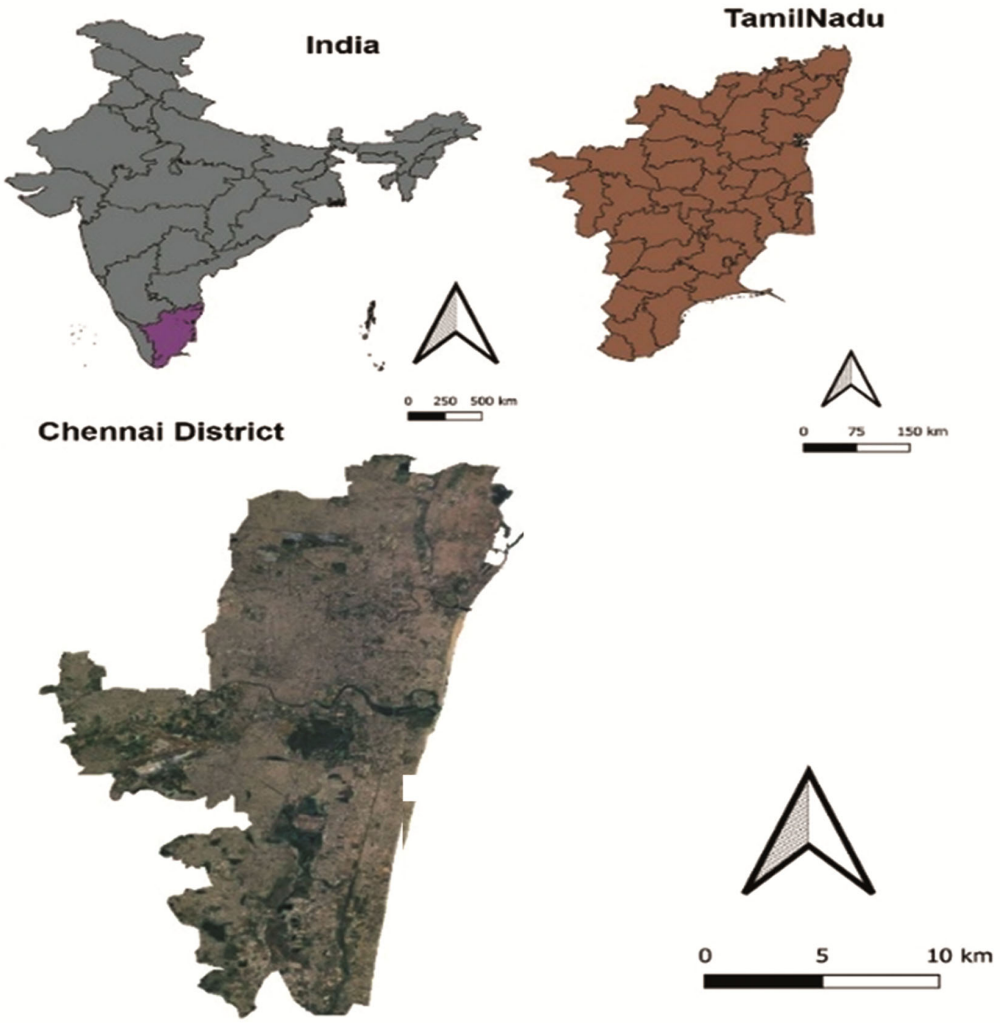

Fig. 1 — Study area map

data, unsupervised learning techniques are preferred for analysing and categorising land changes in this study.

Proposed Methodology

Detailed design about the system architecture of proposed work to analyse and forecast the changes in land is depicted in Fig. 2. Proposed work mainly focuses on two important sub systems: Change detection block and forecasting block. The raw multispectral images are processed and rectified in the pre-processing stage before being passed into the change detection block, which clusters the image data and labels it based on the normalized index values of vegetation, water, and built-up. According to the study region, it is significant to examine urban land areas changes using spectral index values of vegetation, water, and built-up.[21] Pre-processed images are also fed into the forecasting block, which analyses the pre-processed temporal images to forecast the future land image.

Pre-processing

Pixel value of the multispectral image is generally referred as Digital Numbers (DN). The energy measured by satellite sensors may differ from the energy emitted or reflected by a ground surface. The difference is caused by the sun's azimuth, elevation, and atmospheric conditions, which can have an impact on the observed energy. The value recorded in each pixel of the image may include emitted radiation from the surface and emitted radiation from atmosphere also. To identify the properties of land for analysis of land changes only the surface values must be used. Hence, satellite image data is initially pre-processed by performing the atmospheric correction and radiometric correction in raw image data. Radiometric correction reduces or corrects image errors, improving the interpretability and quality of remotely sensed data. The atmospheric correction process[22] eliminates the atmospheric effects on the reflectance values of satellite images.

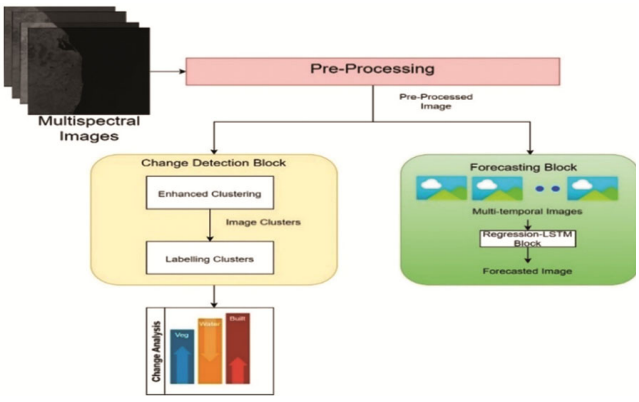

Fig. 2 — Proposed system architecture to analyse and forecast land changes

Pre-processing is carried out for different bands of Landsat8 Multispectral images using the following procedure:

INPUT: Multispectral images.
OUTPUT: Pre-processed multispectral images with surface reflectance

(1) Process individual bands from a multispectral Landsat 8 image.
Read the m x n values in each band for its DN, where $m_{i,j}$ represents the j[th] pixel in the i[th] band.

(2) Perform radiometric corrections and remove the errors introduced due to the atmospheric changes using the following steps

(2.1) Convert the Digital Number values into reflectance with radiometric rescaling coefficients available in Metadata (MTL file) as the DN values are calibrated and scaled when it is acquired by the satellite sensors.

(2.2) Convert the DN values to Top of Atmosphere (TOA) reflectance using Eq. (1)

$$\rho\lambda' = M_\rho Q_{cal} + A_\rho \quad \ldots (1)$$

where, $\rho\lambda'$ indicates the TOA planetary reflectance, without solar angle correction, M_ρ refers to multiplicative rescaling factor specific to the band from the metadata, A_ρ refers to additive rescaling factor specific to the band from the metadata, Q_{cal} refers to Quantized and calibrated standard product pixel values (DN)

(2.3) Compute Sun angle correction for TOA reflectance using Eq. (2)

$$\rho\lambda = \frac{\rho\lambda'}{cos(\theta_{SZ})} = \frac{\rho\lambda'}{\sin(\theta_{SE})} \quad \ldots (2)$$

where, $\rho\lambda$ refers to TOA planetary reflectance, where θ_{SE} denotes Local sun elevation angle in degrees read from metadata, θ_{SZ} denotes Local solar zenith angle $[\theta_{SZ} = 90^\circ - \theta_{SE}]$

(3) Calculate surface reflectance (SR) using the cosine of solar zenith angle correction (COST) model.[20]

(4) Obtain reflectance using radiance values from the satellite sensor using Eq. (3)

(4.1) Convert DN value to spectral radiance using

$$L_{sat} = \left(L_{min} + \frac{L_{max} - L_{min}}{DN_{max}}\right) DN \quad \ldots (3)$$

where, L_{sat} refers to radiance of satellite sensor

(4.2) Convert spectral radiance values to reflectance using Eq. (4)

$$Ref = \pi \left(L_{sat} - L_{haze}\right) / (E_o cos\theta s) \quad \ldots (4)$$

where, L_{haze} refers to Haze radiance, E_o refers to Average(Mean) exoatmospheric spectral solar irradiance on a surface which is perpendicular to the sun's ray, $cos\theta s$ refers to Cosine of solar zenith angle; solar elevation value is found in .MTL file

(5) Repeat steps 2 to 4 for every band.

Firefly Integrated K-means Clustering Algorithm

The Pre-processed and corrected images are then clustered in order to identify the categories of land namely vegetation, water and built-up. K-means being a conventional clustering algorithm for data clustering is often preferred. The limitation in selection of seed point in the initial phase makes it less efficient and also leads to the local convergence problem. Fundamental drawback of K-means algorithm is falling into local optima since it is dependent on the initial centroid values generated randomly. Bio-inspired algorithms which are generally used as optimization techniques have the ability to iteratively search for global optima value.

To improvise the clustering performance, the K-means clustering must have the ability to do two things: find good cluster centroids during initialization, and explore global optima values beyond local optima.

Global optimum in clustering is generally referred as maximizing the intra cluster-similarities within clusters and minimizing the inter cluster-similarities among clusters. Computationally it is difficult to explore the search space in search of global optima without prior information. The K-means approach clusters the data into non-overlapping convex clusters that always converge, just like every partitional clustering algorithm does,[23,24] however it is not always the global optimum. The initial parameters, K, which refers the number of clusters and their centroids, have a significant impact on them. To improve clustering performance, K-means is typically executed multiple times with different random initializations. Each random experiment is conducted in a completely independent manner, and its result cannot be expected as a best one.

Integrating k-means and bio inspired algorithms optimize the results with additional exploration function and it also improvises the current best solution. When a newly discovered solution is enhanced than the current one, the searching agents (fireflies) move to that location, replacing the existing solution, and continue searching until the stopping condition is met. Bio-inspired algorithms are also used to optimize clustering by achieving a higher convergence rate. Three population based bio inspired approaches namely, Firefly Algorithm (FA), ABC and PSO are compared by integrating with k-means to perform clustering task. Integrating k-means clustering with firefly produces improved results since optimal and mean fitness values are produced when compared with the other two bio-inspired algorithms[25] namely ABO and PSO which are taken into consideration.

Firefly Algorithm

Firefly's natural flashing behaviour serves as the inspiration for the Firefly algorithm. In nature, fireflies use their flashes as a signalling mechanism to attract others. Yang *et al.*[26] developed this algorithm using the following key assumptions:

(1) Fireflies are inherently unisex, with a tendency for one firefly to be drawn to another firefly.
(2) The firefly's attractiveness is directly proportionate to the intensity with which it emits light. Among two nearby fireflies, the one with lower brightness moves towards the brighter one. However, brightness diminishes with increasing distance.
(3) If no brighter fireflies are present nearby, a firefly will move in a random direction.

Research shows that FA is mostly used for solving optimization problems and also shows that integrating FA with other techniques produce better performance.[27] Since the FA algorithm primarily uses a population-based approach, it is important to look at the firefly food searching behaviour in order to discover the global optimum. In specific to clustering applications, the initial phase of clustering algorithm involves positioning the fireflies randomly throughout the entire search domain. Fireflies are glow-worms that glow through bioluminescence. Fireflies are physical

entities also termed as agents that carry a luminescence quality which is known as luciferin and will emit light which is directly proportional to this value. The objective function value signifies the integrity of each cluster. The sum of intracluster distances computed between centroids and data points using Euclidean distance metric is used as the objective function of firefly integrated with K-means clustering.

Two Stages of Firefly Algorithm

Variation of Light Intensity:

Values of the objective function are related to light intensity. Assume there is a group of 'n' fireflies, each firefly 'i' is associated with a solution x_i, while its fitness value is represented using $f(x_i)$. The brightness 'L' is determined by the firefly's current position 'x' which corresponds to its fitness value f(x)

$$L_i=f(x_i),\ 1\le i\le n \quad \dots (5)$$

Movement toward Attractive Firefly:

The attractiveness of the firefly is directly proportional to the intensity of light perceived from neighbouring fireflies. Each and every firefly has a distinct attractiveness value (β) which determines its ability to attract others within the group. However, the attractiveness β varies significant based on the distance between fireflies at different locations.

The function β(r), which calculates attractiveness, is computed using Eq. (6).

$$\beta(r) = \beta_0 e^{-\gamma r^2} \quad \dots (6)$$

where, β_0 represents the attractiveness at d=0, γ denotes the light absorption coefficient.

The movement of firefly 'i', positioned at x_i, when attracted to a brighter firefly at x_j, is determined using Eq. (7).

$$x_i(t+1)= x_i(t) + \beta_0 e^{-\gamma r^2}(x_j - x_i) + \alpha b_i \quad \dots (7)$$

where, α indicates randomization coefficient, b_i refers to random numbers which are selected from a Gaussian distribution

Objective Function

Similarity functions (distance measures) are basically used as the objective function for clustering applications. During the initialization phase, the solution space 'S' consists of a finite number of agents, denoted as x_i, where 'i' represents the solution index and i ranges from 1 to N. Each solution 'x', containing a set of centroids, is represented by search agents (fireflies). Using the k-means approach, the centroids can be made use of to grow appropriate clusters over the data points.

Typically, an optimum solution that generates the finest possible configured clusters is sought using a confined population of search agents (fireflies) N, where K denotes the number of clusters. search space's dimension, or D, indicates the amount of attributes each data point can have.

The key objective of the clustering application is to compute the optimal cluster centroids by minimizing te objective function. Centroids are iteratively updated throughout the process, guided by the firefly algorithm, with the expectation that they will gradually converge toward more optimal positions. Optimal configurations of centroids to be computed are found through the following assumptions. Let $w_{i,j}$ represent the weight matrix, $Cen_{j,v}$ represent the centroids of the j^{th} cluster and the v^{th} attribute.

Centroid location can be computed using the clustering objective function as defined in Eq. (9):

$$Wi,j = \begin{cases} 1, & x_i \in cluster_j \\ 0, & x_i \notin cluster_j \end{cases} \quad \dots (8)$$

$$\text{Cenj, v} = \frac{\sum_{i=1}^{s} w_{i,j}x_{i,v}}{\sum_{i=1}^{s} w_{i,j}}\ j = 1..k, v = 1..K \times D \quad \dots (9)$$

$Cen_{j,v}$ is a 2D matrix with K×D dimensions that contains all of the cluster centers.

The distance between x and the cluster centroid is computed based on the attribute values of x within each cluster v, processed through K × D iterations. The objective function used for this study is the Euclidean distance which has to be minimized. It is defined as:

$$F(cen) = \sum_{j=1}^{k}\sum_{i=1}^{s} w_{i,j}\sum_{v=1}^{K\times D}(x_{i,v} - cen_{j,v}) \dots (10)$$

Clustering matrix can be formulated as follows

$$Clmat_{i,j} = \min_{k\in K}\{||x_i - cen_k||\} \quad \dots (11)$$

where, i=1..s , j=1..k , k=1..K. The clustering matrix is optimized to ensure that each data point within a cluster is positioned at the minimum possible distance from its respective centroid.

According to the above equations, the i^{th} data point is assigned to the k^{th} cluster when it's distance between data point and the k^{th} center is at its shortest. The objective function as represented in Eq. (10) indicates that better results are provided with smaller value. An optimized clustering solution is achieved when the objective function reaches its minimum

value, ensuring that all points are as close to their respective centroids as possible.

The objective function value represents the integrity of each cluster. Here, the nature-inspired optimization strategies are used to drive the enhanced clustering process. To ensure the optimal grouping and also to position the data points into a cluster nearest to their centroid, the centroids are shifted at each phase. The primary distinction between original k-mean and firefly integrated k-mean is how the exploration step is implemented to achieve global optimum in the proposed algorithm.[24]

Steps Involved in Integrating Firefly Algorithm with K-means Clustering

(1) Initialization phase
- (1.1) Import the data for clustering from multispectral image represented as B_{ij} where i=1 to n, i represents the pixel values from each band and j=1 to D (D=4, representing 4 bands).
- (1.2) Initialize number of clusters (K), firefly population size (N) and other initial parameters such as β, α and γ
- (1.3) Initialize each firefly with random K × D cluster centers

(2) Exploration phase
- (2.1) Determine the fitness of each firefly's centroid and adjust its light intensity according to the fitness values using Eq. (5)
- (2.2) For all the fireflies (i= 1 to N) when compared with other fireflies (j=1 to N), check the brightness of firefly 'i' and 'j'. Move the fireflies using Eq. (7).
- (2.3) Proceed with updating cluster centroids and cluster assignment phase

(3) Centroids Updation and Cluster assignment
- (3.1) Update cluster centers based on the updated position of the firefly.
- 3.2) Compute fitness of new solution and update the light intensity, if it is better proceed with next step.
- (3.3) Rank the fireflies and identify the optimized best solution.
- (3.4) Reassign data points from dataset to the optimized cluster centers.
- (3.5) Output the optimized cluster centers which is represented by firefly with best fitness value

Enhanced clustering integrates the K-means algorithm with the Firefly Algorithm to optimize cluster centroids efficiently.

To denote an image with a limited number of meaningful segments instead of thousands of individual pixels, the image undergoes partitioning. Additionally, partitioning the image into segments can be viewed as a clustering method in which pixels meeting a criterion are grouped together into the same cluster, while those that don't meet the criterion are assigned to separate cluster. One popular method for addressing the difficulties associated with learning from unlabelled data is to first group the data according to specific measures of similarity or dissimilarity, and then label each group.[28]

Labelling the Clusters

To identify the land categories, the cluster groups generated in the preceding phase must be labelled. The clusters are identified using a standard index, such as the normalised difference index, which labels the land as vegetation, water, and built-up areas. The intensity values of vegetation, water, and buildings are calculated using the NDWI, NDBI and NDVI for Multispectral images that include temporal data from the same geographic location.[14,29] For each of the clusters, the mean NDWI, NDVI, and NDBI values are individually determined, and the cluster with the highest average of these values is labelled as vegetation, water, or a building, respectively. The computation of these index values are listed below:

NDVI

NDVI[30,31] is a commonly used metric in remote sensing to identify vegetated regions. This metric illustrates the higher reflectance of near-infrared light in comparison to visible red light. It also helps to separate bare soil from grass or a forest and different types of crops.

$$\mathrm{NDVI} = \frac{NIR - RED}{NIR + RED} \quad \ldots (12)$$

The normalized difference between red and near-infrared bands is termed as the NDVI.

NDBI

NDBI[32] metric is generally used to map urban built-up areas from the remote sensing multispectral images because of their ability to provide accurate information about urban land cover.

$$\mathrm{NDBI} = \frac{\mathrm{SWIR} - \mathrm{NIR}}{\mathrm{SWIR} + \mathrm{NIR}} \quad \ldots (13)$$

NDBI is the normalized difference of short wave infrared and near-infrared.

NDWI

NDWI[33,34] is a technique to enhance the appearance of the open water feature in remotely sensed digital imagery. Experts can also estimate the turbidity of water bodies using remotely sensed water bodies. Water bodies have a low reflectance, hence the electromagnetic spectrum's visible region is where it reflects.

$$\text{NDWI} = \frac{Green - SWIR}{Green + SWIR} \quad \ldots (14)$$

Land Use and Land Cover Change

Changes in land usage and cover are analysed to show how the land has changed through time. Pixel-based comparison studies are carried out to generate change information on a pixel basis, which more effectively interprets changes based on prior knowledge. Comparisons between the successive periods of time were conducted to highlight the differences between the periods after identifying the clusters to interpret the conditions of the land throughout years. Using the following formulae Eqs (15) and (16), the percentage of change and rate of change were also estimated to show the magnitude of the changes experienced between the periods.[35]
Analysis of land regions are calculated by computing the percentage of Vegetation, Water and Building areas in the land Eq. (15)

$$\text{Percentage of Land regions} = I/T * 100 \quad \ldots (15)$$

where, T denotes total count of pixels present in the image, while I represent the total number of pixels covered by the Vegetation, Water, and Building regions.

Rate of change in land regions over a year are computed using Eq. (16).

$$\text{Rate of change} = T_2 - T_1 \quad \ldots (16)$$

where, T_2 represents Current year image and T_1 represents past year image.

Prediction of Land Area

Forecasting the future image, involves processing the past pixel values taken from multi-temporal images and predicting the new pixel values of each band. Each band was extracted at different times in the same geographic location. Regression LSTM network has been applied in this work to predict the future land area. Then the forecasted image is clustered to analyse the regions of land.

Defining LSTM Network

To forecast the future image LSTM has been used, multi-temporal images are fed as input to LSTM network. The input for LSTM is given by taking the pixel values from different band images captured over different periods (i.e.) the first pixel value of the first band for the first year, the first pixel value of the first band for the second year, the first pixel value of the first band for the third year and so on are considered as a sequence, and the respective pixel value for the first band is calculated for the near future after giving it as an input to the LSTM. Likewise, all the band values for the future year are calculated. LSTM network architecture is designed as specified in Table 1, and the model is trained with the parameters as mentioned in Table 2.

Algorithm

Input: Load Sequence of Multi-Temporal pre-processed Multispectral image

Output: Forecasted image

Step-1– Read the multitemporal images (Tb_{11}, Tb_{12}, Tb_{13}, Tb_{14}, Tb_{21}, Tb_{22}, Tb_{23}, Tb_{24}, Tb_{31}, Tb_{32}, Tb_{33}, Tb_{34}, Tb_{41}, Tb_{42}, Tb_{43}, Tb_{44} …) where, Tb_{ij} represents the i^{th} band of the j^{th} year.

Step-2 – For the first band, define a layer array (4 × 1) which includes sequence input layer, LSTM layer, fully connected layer and regression output layer as per the design specification shown in Table 1

Step-3 – Train the network with the parameters shown in Table 2 and predict the initial response using a trained model. Then, by looping over the

Table 1 — LSTM network architecture

Layer	Specification
Sequence input layer	1 Four year band information
LSTM layer	200 – hidden units
Fully connected layer	1
Regression layer	Half mean squared error loss

Table 2 — Training parameters

Parameter	Value
Number of epochs	100
Optimizer	Adaptive moment estimation (Adam)
Learning rate	0.05
Gradient Threshold	1
Learning rate drop factor	0.2

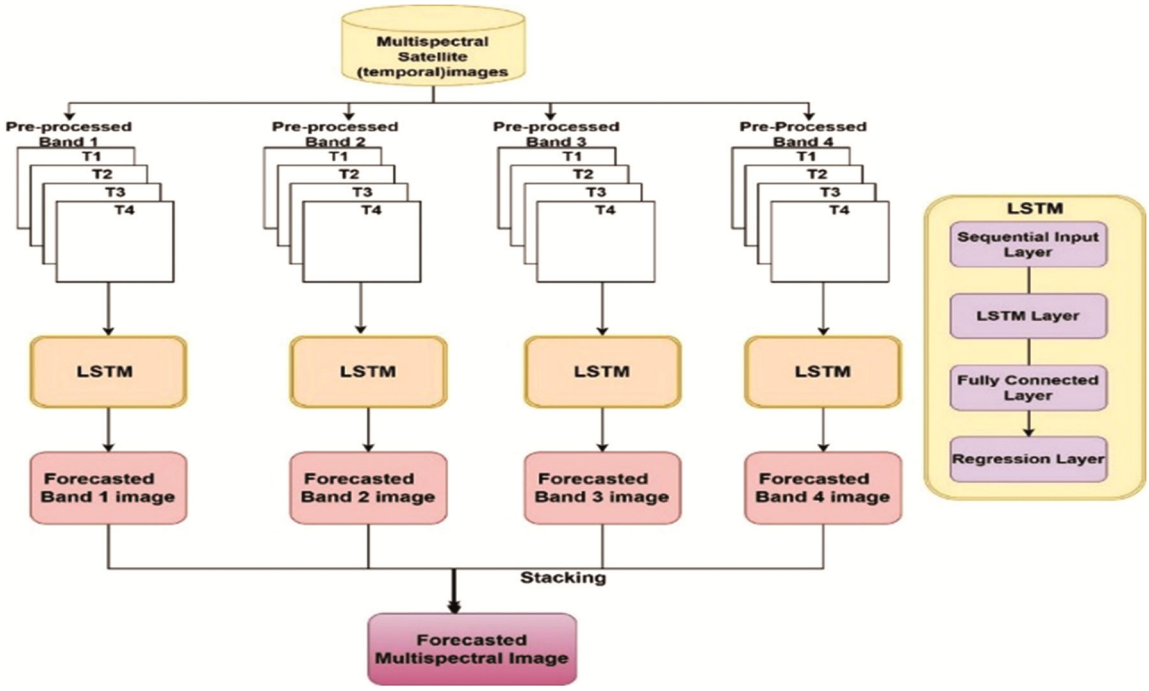

Fig. 3 — LSTM-based multi-spectral temporal forecasting

epochs, update the network state, which forecasts the subsequent response.

Step-4 – Repeat the steps two and three for the remaining bands of multispectral image

Step-5 – Stack the forecasted bands to form forecasted multispectral image.

The detailed flow of LSTM based Multispectral temporal forecasting approach is presented in Fig. 3. This includes processing spectral bands of temporal images, training the LSTM network for each band with temporal variations across years represented as T1, T2, T3 and T4 respectively and further forecasting the future spectral bands.

Experimental Setup

The experiments are conducted in system configuration of HP Intel(R) Core(TM) i7-7700 processor @3.60GHZ, with 16 GB Installed RAM, Dedicated 2.0 GB NVIDIA GeForce GT 730 GPU and 1 TB Hard disk. Entire experimentation is implemented in Matlab (R2018a) environment. The parameters set for Firefly integrated k-means clustering approach are reported in Table 3.

Results and Discussion

When exporting USGS multispectral image data from Earth Explorer, a region's name or latitude and longitude could be used to specify the region.

Table 3— Parameters set for Firefly integrated k-means clustering ap

Parameter	Value
Number of fireflies	20
Number of clusters	3
Attractiveness	1
Absorption	1
Randomness	0.2

Multispectral data includes 11 bands of image (Coastal -Band 1, Blue - Band 2, Green - Band 3, Red – Band 4, Near-Infrared NIR – Band 5, Short wave infrared (SWIR1) – Band 6, SWIR 2 - Band 7, Panchromatic - Band 8, Cirrus - Band 9, TRIS 1 - Band 10, TRIS 2 - Band 11) and metadata file (MTL) by which corrections can be carried out for calibrated data from sensors. Selective bands that are necessary for this work are chosen, and the raw image is processed in order to analyse it for Land use and Land cover. Processing is done on Landsat 8's four bands [14,29] which include Band 3, Band 4, Band 5, and Band 6.

Raw Data

The four bands extracted for this work namely band 3(green), band 4(red), band 5(NIR) and band 6(SWIR1) from a sample multispectral image are shown in Fig. 4.a

Pre-Processed Bands

Extracted bands shown in Fig. 4(a) are pre-processed and corrected for radiometric and

atmospheric corrections and the results of pre-processing are shown in Fig. 4(b).

Firefly Integrated K-means Clustering Algorithm

The pre-processed multispectral images are further analysed to cluster the regions in land using Firefly integrated k-means clustering approach. Fig. 4.c demonstrates the clustering results, and the clusters are labelled using the indexes specified in the section labelling the clusters respectively.

Regression LSTM network is applied for forecasting images, and when the network is trained using pre-processed temporal bands, each band's expected pixel values are computed. Individual bands are predicted, and all bands are stacked to create a multispectral layered image that is validated using pixel Structural SIMilarity (SSIM) index as defined by Eq. (17).

$$SSIM(a,b)=[l(a,b)]^{\alpha}\cdot[c(a,b)]^{\beta}\cdot[s(a,b)]^{\gamma} \quad \ldots (17)$$

where, l indicates the luminance, c represents the contrast, and s represents the structure which denotes the local pattern between pair of images to identify the similarity and dissimilarity and α, β and γ are positive constants.

Using Firefly integrated K-means clustering approach, the predicted image is also clustered and examined for identifying changes in the land. The actual multispectral image and results of clustering and labelling of both the actual multispectral image and the forecasted image are presented in Fig. 5. The

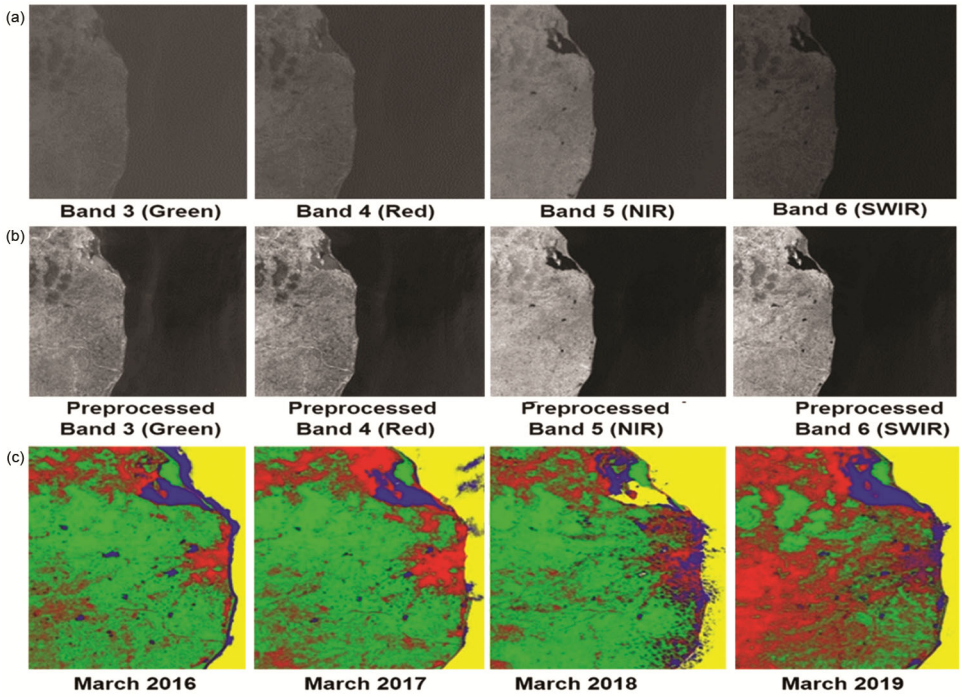

Fig. 4 — Sample input bands and their results: (a) Sample Landsat 8 bands, (b) Sample preprocessed Landsat 8 bands, (c) Stacked multitemporal images of same geographical location after applying enhanced clustering approach

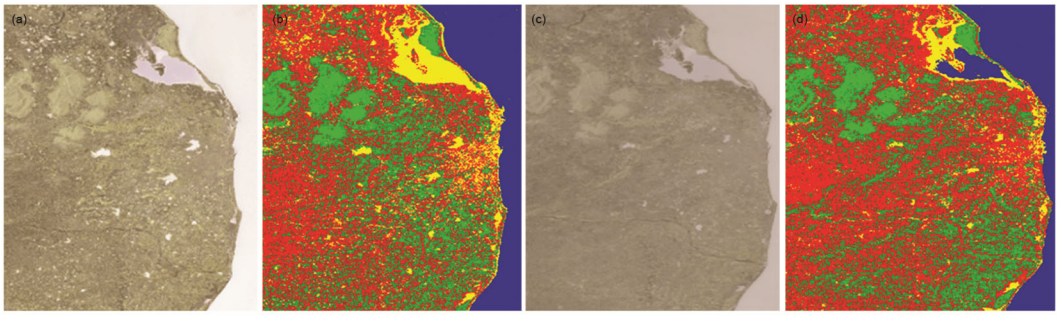

Fig 5 — Actual vs predicted result using LSTM: (a) Actual Multispectral Image, (b) After clustering, (c) Forecasted Image, (d) After Clustering of forecasted image

Table 4 — Computation of Intracluster distance - Traditional K-means and Firefly integrated K-means clustering

Technique	Intracluster Distance in cluster 1	Intracluster Distance in cluster 2	Intracluster Distance in cluster 3	Total Distance
K means	23.34	21.47	28.34	73.16
Firefly integrated K-means Clustering	19.0	24.0	19.65	63.64

labelled images are used to analyse the land use and land cover regions.

The Firefly integrated k-mean Clustering approach is compared against the conventional K-means algorithm by comparing the intra cluster distance of each cluster that specifies the land, vegetation, and water areas for both K-means and firefly integrated K-means clustering methods. The overall cluster distance is calculated by adding the intra cluster distance for each point in the land region cluster from the respective cluster centers.

As stated in the Table 4, the total intra cluster distance for Firefly integrated K-means is lesser than that of the traditional K means algorithm which is in accordance with the objective which is to minimize the distance of the data point from its cluster center.

It's concluded that proposed enhanced clustering technique performs better than the traditional K-means clustering algorithm. A pixel's distance from its cluster center is computed to determine how well a pixel is connected with a cluster. The data recorded for each pixel is typically a combination of the spectral responses present in the pixel's corresponding area. Anomalies are detected during the clustering phase; even pure class pixels can be spectral response mixtures from other spectral clusters.[36] Deviations in intracluster distance computation, on the other hand, arise as a result of the mixed pixel problem in remote sensing data. Because of data acquisition constraints and the mixed pixel effect, some clusters may have some uncertainties whereas others do not.

Different techniques are utilized to evaluate clustering results, but unlike most performance assessment methods that require a training set, the Silhouette index does not require training set.[28] The Silhouette index[37,38] is used to evaluate the performance of the traditional K-means clustering approach and Firefly integrated K-means clustering approach presented in this work.

$$\text{Silhouette Coefficient} = (p-q)/\max(p,q) \quad \ldots (18)$$

where, q is the average distance between each instance within the cluster. p denotes the average distance to the instances of the next closest cluster. The range of coefficient is −1 to 1. The instance belongs to the correct cluster and is in close proximity to its cluster if the value is near 1. A value close to −1, however, indicates that the value has been allotted to the incorrect cluster.

Table 5— Average Silhouette index value

Clustering Method	No of Clusters	Value
K-means Clustering	3	0.88
Firefly integrated K-means clustering	3	0.93

Table 6 — Analysis of land regions

Sl. No	Year	Built-up (%)	Vegetation (%)	Water (%)
1	2016	33.57	60.3	6.06
2	2017	36.91	58.22	4.77
3	2018	32.95	59.29	7.67
4	2019	53.98	37.59	8.34

Average silhouette value obtained for the proposed approach and traditional K-means clustering approach is listed in Table 5.

Rate of Change in Land Use and Land Cover

To analyse the areas of land over years, the land cover and land use changes in percentage over years are computed from multi-temporal images using Eq. (15) and shown in Table 6. The rate of change in vegetation, water and built-up areas over a year is depicted in Table 7.

The changes in land region over the years are visually depicted in Fig. 6

The similarity between the forecasted image from the Regression LSTM network and the original image after pre-processing is evaluated. The land regions have been evaluated by performing enhanced clustering on forecasted image and pre-processed image as well. Exact pixel differences between two images has been evaluated using the SSIM.[39] Similarity of actual image and predicted image are measured using Root Mean Square Error (RMSE). When the forecasted images are stacked into a multispectral image a SSIM of 0.85 and a RMSE of 0.41 has been achieved. The proposed architecture uses enhanced clustering to identify the changes in land by categorizing the clusters based on the vegetation, water and building indexes. This model works effectively than popular K-means algorithm for clustering, but due to the seasonal changes in real

Table 7 — Rate of change over year

Sl. No	Year		Rate of Change		
	From	To	Built-up (%)	Vegetation (%)	Water (%)
1	2016	2017	3.34	−2.08	−1.29
2	2017	2018	−3.96	1.07	2.9
3	2018	2019	21.03	−21.7	0.67
Average rate of change (2016-2019)			6.80	7.57	0.76

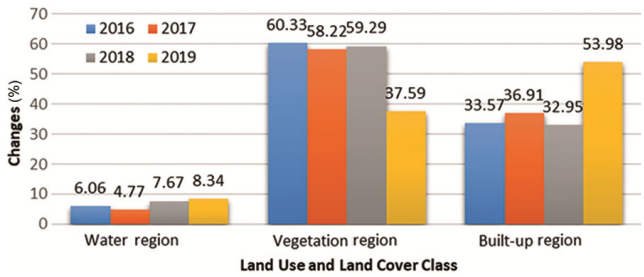

Fig. 6 —Change of land regions

time dataset few outliers occur in clustering approach.[40]

Conclusions

Land regions are clustered for change detection using enhanced clustering, with each cluster labelled based on Normalized Difference Indices like NDVI, NDWI, and NDBI. Integrating the Firefly algorithm with K-means optimizes centroid positioning, reducing intra-cluster distance and enhancing spatial coherence while minimizing uncertainties. A high Silhouette index ensures compact, well-separated clusters, while regression LSTM-based forecasting achieves accurate multispectral predictions. High structural similarity and low error rates validate the model's effectiveness in capturing spatiotemporal land cover changes. Land cover assessment was improved by analysing vegetation, water, and built-up area percentages over time Cloud-free data acquisition and mixed pixels from land cover transitions and sub-pixel targets introduced clustering uncertainties, which can be reduced through subpixel mapping for better spectral cluster refinement and intra-cluster compactness. Future enhancements include deep learning-based feature extraction to improve prediction accuracy. The work has significant applications in land use monitoring, environmental assessment, and urban planning, aiding geospatial decision-making.

Conflicts of Interest

The author(s) state that there are no conflicts of interest to disclose with the current work.

Acknowledgment

Financial support for this work comes from the DeitY-Visvesvaraya PhD Scheme for Electronics and IT fellowship.

References

1 Islam K, Jashimuddin M, Nath B & Nath T K, Land use classification and change detection by using multi-temporal remotely sensed imagery: The case of chunati wildlife sanctuary, Bangladesh, *Egypt J Remote Sens Space Sci*, **21(1)** (2018) 37–47, https://doi.org/10.1016/j.ejrs.2016.12.005.

2 Clark M L, Mapping land cover with hyperspectral and multispectral satellites using machine learning and spectral mixture analysis, in *IEEE Int Geosci Remote Sens Symp (IGARSS)*, 2016, 513–516, https://doi.org/10.1109/IGARSS.2016.7729127.

3 Sundara K K, Valasala S S N V A, Subrahmanyam J V V, Mallampati M, Shaik K & Ekkirala P, Prediction of future land use land cover changes of vijayawada City using remote sensing and GIS, *Int J Innov Res Adv Eng*, **2(3)** (2015) 91–97.

4 Kumar S, Shwetank and Jain K, A multi-temporal Landsat data analysis for land-use/land-cover change in haridwar Region using remote sensing techniques, *Procedia Comput Sci*, **171** (2020) 1184–1193, https://doi.org/10.1016/j.procs.2020.04.127.

5 Sharma D & Kundra H, Hybrid algorithm of particle swarm optimization and firefly for natural terrain feature extraction, *Int J Comput Sci Inf Secur*, **14(12)** (2016).

6 Li L, Zhang B & Li J, Statistically modelling and mining remotely sensed data in urban areas based on topic models—a conceptual analysis, *2016 8th Workshop Hyperspectral Image Signal Process Evol Remote Sens (WHISPERS)*, 2016, 1–5, https://doi.org/10.1109/WHISPERS.2016.8071764.

7 Kumar S & Arya S, Change detection techniques for land cover change analysis using spatial datasets: a review, *Remote Sens Earth Syst Sci*, **4(3)** (2021) 172–185, https://doi.org/10.1007/s41976-021-00056-z

8 Duong N D, Hang L M, Tuan T A & Ouyang Z, Development of a spectral-pattern-analysis-based method for automated water body extraction using Landsat image data: a case study in central vietnam and southern laos, *Limnol Oceanogr Methods*, **15(11)** (2017) 945–959, https://doi.org/10.1002/lom3.10215.

9 Shang Z & Hamerlinck J D, Using statistics and spatial data mining to study land cover in wyoming: can we predict vegetation types from environmental variables?, in *Seventh IEEE Int Conf Data Min Workshops (ICDMW 2007)*, 2007, 661–666, https://doi.org/10.1109/ICDMW.2007.87.

10 Uehara K, Nosato H, Murakawa M, Nakamura R, Miyamoto H & Sakanashi H, Multi-channel higher-order local autocorrelation for object detection on satellite images, *Int J Remote Sens*, **41(2)** (2020) 752–771, https://doi.org/10.1080/01431161.2019.1648904.

11 Paul S & Kumar N D, Evaluation of feature selection and feature extraction techniques on multi-temporal landsat-8 images for crop classification, *Remote Sensing in Earth Systems Sciences*, **2(4)** (2019) 197–207, https://doi.org/10.1007/s41976-019-00024-8.

12 Marnur A M. & Gavade A B, Satellite image classification and feature extraction using various classification techniques: a survey, *Int. J. Adv. Res. Ideas Innov. Technol*, **4(3)** (2018) 2454–3132, https://doi.org/10.13140/RG.2.2.20964.94084.

13 Neagoe V-E & Chirila B V, A new approach to unsupervised classification of hyperspectral earth observation imagery using a Gaussian mixture model, *Int J Signal Process,* **1** (2016) 134–137.

14 Taufik A, Ahmad S S S & Khairuddin N F E, Classification of landsat 8 satellite data using fuzzy c-means, in *Proc 2017 Int Conf Mach Learn Soft Comput*, 2017, 58–62, https://doi.org/10.1145/3036290.3036330.

15 Senthilnath J, Kulkarni S, Benediktsson J A & Yang X S, A novel approach for multispectral satellite image classification based on the bat algorithm, *IEEE Geosci Remote Sens Lett*, **13(4)** (2016) 599–603, https://doi.org/10.1109/LGRS.2016.2530724.

16 Goel S, Gaur M & Jain E, Nature inspired algorithms in remote sensing image classification" *Procedia Comput Sci*, **57** (2015) 377–384, https://doi.org/10.1016/j.procs.2015.07.352.

17 Joshil R K & SivaSathya S, A survey of various algorithms used on multispectral satellite image classification of alwar image dataset, *Indian J Sci Technol*, **9(45)** (2016) 1–11, https://doi.org/10.17485/ijst/2016/v9i45/105304.

18 Nayak, J, Naik B & Behera H S, A novel nature inspired firefly algorithm with higher order neural network: performance analysis, *Eng Sci Technol Int J,* **19(1)** (2016) 197–211, https://doi.org/10.1016/j.jestch.2015.07.005.

19 Goel L, Gupta D & Panchal V K, Hybrid bio-inspired techniques for land cover feature extraction: A remote sensing perspective, *Appl Soft Comput*, **12(2)** (2012) 832–849, https://doi.org/10.1016/j.asoc.2011.10.006.

20 Landsat 8 https://earthexplorer.usgs.gov/

21 Sharma R C, Hoan T N, Saeid G, Bai X, Nguyen L V & Tateishi R, Spectral features for the detection of land cover changes, *J Geosci Environ Prot*, **7(05)** (2019) 81, https://doi.org/10.4236/gep.2019.75009.

22 Chavez P S, Image-based atmospheric corrections-revisited and improved, *Photogramm Eng Remote Sens*, **62(9)** (1996) 1025–1035.

23 Hailun X, Zhang L, Lim C P, Yu Y, Liu C, Liu H & Walters J, Improving K-means clustering with enhanced firefly algorithms," *Appl Soft Comput*, **84** (2019) 105763, https://doi.org/10.1016/j.asoc.2019.105763.

24 Tang R, Fong S, Yang X-S & Deb S, Integrating nature-inspired optimization algorithms to K-means clustering, in *Seventh Int Conf Digit Inf Manag (ICDIM 2012)*, 2012, 116–123, https://doi.org/10.1109/ICDIM.2012.6360145

25 Senthilnath J, Omkar S N & Mani V, Clustering using firefly algorithm: performance study, *Swarm Evol Comput,* **1(3)** (2011) 164–171, https://doi.org/10.1016/j.swevo.2011.06.003

26 Yang X S & He X S, Why the firefly algorithm works?, *Nat-Inspired Algorithms Appl Optim*, 2018, 245–259, https://doi.org/10.1007/978-3-319-67669-2_11.

27 Johari N F, Zain A M, Noorfa M H & Udin A, Firefly algorithm for optimization problem, in *Appl Mech Mater*, **421** (2013) 512–517, https://doi.org/10.4028/www.scientific.net/AMM.421.512.

28 Mittal H, Pandey A C, Saraswat M, Kumar S, Pal R & Modwel G, A comprehensive survey of image segmentation: clustering methods, performance parameters, and benchmark datasets, *Multimed Tools Appl*, (2022) 1–26, https://doi.org/10.1007/s11042-021-10594-9.

29 Yu Z, Di L, Yang R, Tang J, Lin L, Zhang C, Rahman Md S, Zhao H, Gaigalas J, Yu E G & Sun Z, Selection of Landsat 8 OLI band combinations for land use and land cover classification, in *8th Int Conf Agro-Geoinformatics (Agro-Geoinformatics),* 2019, 1–5, https://doi.org/10.1109/Agro-Geoinformatics.2019.8820595.

30 Rouse J W Jr, Haas R H, Schell J A & Deering D W, Monitoring vegetation systems in the Great Plains with ERTS, *NASA Spec Publ*, **351(1)** (1974) 309.

31 Fung, T & Siu W, Environmental quality and its changes, an analysis using NDVI, *Int J Remote Sens,* **21(5)** (2000) 1011–1024, https://doi.org/10.1080/014311600210407.

32 Zha, Y, Gao J & Ni S, Use of normalized difference built-up index in automatically mapping urban areas from TM imagery, *Int J Remote Sens*, **24(3)** (2003) 583–594, https://doi.org/10.1080/01431160304987

33 Gao B C, NDWI—A normalized difference water index for remote sensing of vegetation liquid water from space, *Remote Sens Environ*, **58(3)** (1996) 257–266, https://doi.org/10.1016/S0034-4257(96)00067-3

34 Özelkan E, Water body detection analysis using NDWI indices derived from landsat-8 OLI, *Pol J Environ Stud*, **29(2)** (2020) 1759–1769, https://doi.org/10.15244/pjoes/110447

35 Othow O O, Gebre S L & Gemeda D O, Analyzing the rate of land use and land cover change and determining the causes of forest cover change in GOG district, Gambella regional state, Ethiopia, *J Remote Sens GIS*, **6(4)** (2017) 218, https://doi.org/10.4172/2469-4134.1000219.

36 Duran O & Petrou M, Spectral unmixing with negative and superunity abundances for subpixel anomaly detection, *IEEE Geosci Remote Sen Lett*, **6(1)** (2008) 152–156, https://doi.org/10.1109/LGRS.2008.2009952

37 Shutaywi M & Kachouie N N, Silhouette analysis for performance evaluation in machine learning with applications to clustering, *Entropy*, **23(6)** (2021) 759, https://doi.org/10.3390/e23060759

38 Shahapure K R & Nicholas C, Cluster quality analysis using silhouette score, in *2020 IEEE 7th Int Conf Data Sci Adv Anal (DSAA)*, 2020, 747–748, https://doi.org/10.1109/DSAA49011.2020.00096.

39 Biró L, Kozma-Bognár V & Berke J, Comparison of RGB indices used for vegetation studies based on structured similarity index (SSIM), *J Plant Sci Phytopathol*, **8(1)** (2024) 007–012, https://dx.doi.org/10.29328/journal.jpsp.1001124.

40 Atif M, Farooq M, Shafiq M, Alballa T, Alhabeeb S A & Khalifa H A E-W, Uncovering the impact of outliers on clusters' evolution in temporal data-sets: an empirical analysis, *Sci Rep*, **14** (2024) 30674, https://doi.org/10.1038/s41598-024-75928-7.